Original Research

Nucleated red blood cells participate in myocardial regeneration in the toad *Bufo Gargarizan Gargarizan*

Shu-Qin Liu[1], Xiao-Ye Hou[1], Feng Zhao[2] and Xiao-Ge Zhao[3]

[1]Department of Pharmacology, School of Basic Medical Sciences, Xi'an Jiaotong University Health Science Center, Xi'an 710061, China; [2]The Basic Medical Central Laboratory, School of Basic Medical Sciences, Xi'an Jiaotong University Health Science Center, Xi'an 710061, China; [3]The Central Laboratory For Biomedical Research, Xi'an Jiaotong University Health Science Center, Xi'an 710061, China
Corresponding author: Shu-Qin Liu. Email: lsq@xjtu.edu.cn

Impact statement

Heart regeneration is negligible in mammals but remarkable in ectotherms, and this has been attributed to fewer cardiomyocytes (CMs) in mammalian hearts, in contrast to an abundance of CMs in ectotherms' hearts, retaining proliferative potentials. Nucleated red blood cells (NRBCs) are rare in mammalian blood, but are abundant in ectotherms' blood. Here we found toad NRBCs participating in CMs renewal/regeneration: CM loss triggered a series of biological processes, inducing NRBC infiltration and transition to CM; NRBC infiltration pause due to NRBC supply suspension delayed myocardial regeneration. This finding implies that the lack of NRBCs is a reason for the limited human heart regeneration. Toad dominant NRBCs are related to the low blood partial pressure of O_2. For humans, the hypoxic microenvironment in infarcted myocardium may be suitable for NRBCs to survive and transdifferentiate into CMs. Hence, utilizing bone marrow NRBCs is a potential strategy to enhance human myocardial regeneration.

Abstract

Heart regeneration is negligible in humans and mammals but remarkable in some ectotherms. Humans and mammals lack nucleated red blood cells (NRBCs), while ectotherms have sufficient NRBCs. This study used *Bufo gargarizan gargarizan*, a Chinese toad subspecies, as a model animal to verify our hypothesis that NRBCs participate in myocardial regeneration. NRBC infiltration into myocardium was seen in the healthy toad hearts. Heart needle-injury was used as an enlarged model of physiological cardiomyocyte loss. It recovered quickly and scarlessly. NRBC infiltration increased during the recovery. Transwell assay was done to *in vitro* explore effects of myocardial injury on NRBCs. In the transwell system, NRBCs could infiltrate into cardiac pieces and could transdifferentiate toward cardiomyocytes. Heart apex cautery caused approximately 5% of the ventricle to be injured to varying degrees. In the mildly to moderately injured regions, NRBC infiltration increased and myocardial regeneration started soon after the inflammatory response; the severely damaged region underwent inflammation, scarring, and vascularity before NRBC infiltration and myocardial regeneration, and recovered scarlessly in four months. NRBCs were seen in the newly formed myocardium. Enzyme-linked immunosorbent assay and Western blotting showed that the levels of tumor necrosis factor-α, interleukin- 1β, 6, and11, cardiotrophin-1, vascular endothelial growth factor, erythropoietin, matrix metalloproteinase- 2 and 9 in the serum and/or cardiac tissues fluctuated in different patterns during the cardiac injury-regeneration. Cardiotrophin-1 could induce toad NRBC transdifferentiation toward cardiomyocytes *in vitro*. Taken together, the results suggest that the NRBC is a cell source for cardiomyocyte renewal/regeneration in the toad; cardiomyocyte loss triggers a series of biological processes, facilitating NRBC infiltration and transition to cardiomyocytes. This finding may guide a new direction for improving human myocardial regeneration.

Keywords: Nucleated red blood cell, myocardial regeneration, cardiomyocyte, toad, *Bufo gargarizan gargarizan*, model animal

***Experimental Biology and Medicine* 2021; 246: 1760–1775. DOI: 10.1177/15353702211013297**

Introduction

Heart disease remains one of the major causes of morbidity and mortality worldwide. After injury, human hearts show a negligible ability to regenerate cardiomyocytes (CMs), so the damaged myocardium will be replaced by scar tissue, which limits the diastolic and contractile function of adjacent myocardium, causes arrhythmia, heart failure, and death.[1] Mammals studied are similar to humans.[2] Mammalian CMs cease their cell-cycle shortly after birth and cardiac injury may accelerate the cessation.[3,4] However, CM renewal occurs throughout life, and its rate is very low and decreases with age.[5,6] Further studies have

shown that the CM renewal[7] and the CM regeneration after injury[8,9] were accompanied by few existing CMs reentering the cell cycle. Therefore, the current mainstream understanding of human CM renewal/regeneration is that few CMs retain the proliferative potential,[2,7,9] and this has led to cardiac regeneration research focusing on CM cell-cycle arrest and reentry.[2] However, the outcome of cell cycle activity is not necessarily CM division but instead can be one of many possibilities.[10] Meanwhile, entire heart snRNA-seq (single-nucleus sequencing) analyses have revealed nascent CMs with specific markers of other cell types in hearts of neonatal and adult mice.[11,12] Is there any other cell source for the CM renewal/regeneration?

Actually, several adult stem cell populations, including hematopoietic stem/progenitor cells, have been shown to possess cardiac regenerative potential,[13–18] although results from different research groups have appeared diverse.[15] In addition, some progress has been made in artificial transdifferentiation of cardiac fibroblasts into CMs.[19,20] So far there is no report of endogenous transition of CMs from non-CMs other than stem cells.

Interspecies- and intraspecies comparisons may provide clues for exploring cardiac regeneration. Many teleosts and amphibians show a remarkable capacity to regenerate CMs, and its mechanism has also been documented as proliferation of existing CMs.[1,2,21–25] Thus, the difference in the capacity of cardiac regeneration between mammals and ectotherms is being interpreted as the difference in the number of proliferative CMs.[2] An array of biological comparison-based studies have revealed many genes, signaling cascades, as well as metabolic and environmental factors that play key roles in myocardial regeneration.[2] However, little attention has been paid at the cell level.

Red blood cells (RBCs) differ greatly between ectotherms and humans and mammals. For ectotherms, almost all circulatory RBCs are nucleated RBCs (NRBCs), which is related to these animals' low blood partial pressure of O_2 due to their slow body metabolisms.[2] For humans, NRBCs are normally present in fetal blood and in neonatal blood ($0.5–1.1 \times 10^9$ L^{-1}), but disappear shortly after birth.[26] It is difficult to find NRBCs in older childrens' blood. Circulatory RBCs in healthy adult humans and mammals are nuclear-free. NRBCs may, however, appear in the blood of adults who are in pregnancy[27] or are suffering from diseases such as chronic hypoxia, anemia, and surgical sepsis.[28,29]

Interestingly, the abundant NRBCs in ectotherms are in line with the remarkable capacity to regenerate CMs. For humans and mammals, fetuses and neonates do possess an ability to regenerate CMs, with this ability being lost within a short time after birth,[30–32] and the maternal heart can adaptively grow with the fetal growth,[33] corresponding well temporally to the changes of circulatory NRBCs. Systemic hypoxia induced cardiac regeneration in adult mice;[8] and hypoxia in parturient rats led to increased circulatory NRBCs in their neonatal rats.[34] It is generally thought that the increased NRBCs and myocardial regeneration are two independent events following hypoxia. Apart from transporting O_2 and CO_2, it is unknown whether NRBCs play a direct role in myocardial regeneration. Clinicopathological examinations showed the appearance of NRBCs in the pericardial fluid of one neonate with cyanotic congenital heart disease[35] and in the granulation tissue or peri-granulation tissue of three adult hearts after myocardial infarction.[36] We hypothesize that NRBCs directly participate in myocardial regeneration.

Human bone marrow (BM) NRBCs include pronormablasts, basophilic normablasts, polychromatophilic normablasts, and orthochromatic normablasts, respectively accounting for 0.57%, 0.92%, 7.41%, and 10.75% of total BM-nucleated cells (Chinese data, Chinese Academy of Medical Sciences Institute of Blood Transfusion and Hematology, 1963), and the orthochromatic normablast is close to the mature RBC in hemoglobin (Hb) content and cannot divide.[37] We estimate NRBCs that can enter into the blood are most likely the orthochromatic- and polychromatophilic normablasts.

So far there is no report of toad heart regeneration. *Bufo gargarizans* also known as Chinese toads are widely distributed in China, Russia, and the Korean Peninsula. There are both NRBCs and mature RBCs in *Bufo gargarizans*' blood, in which NRBCs account for more than 99% of total RBCs and are rich in Hb, are large in size, and the overwhelming majority of which do not divide (Data in Chinese, Guo *et al.*, 2002). We speculate that *Bufo gargarizans* NRBCs are equivalent to human orthochromatic normablasts. Here we used *Bufo gargarizan gargarizan*, a Chinese toad subspecies, as a model animal to test our hypothesis. We find that the toad NRBC is a cell source for CM renewal/regeneration. Also, we show for the first time NRBC infiltration into myocardium in the healthy vertebrate.

Materials and methods

Animals and ethics statement

Male *Bufo gargarizan gargarizans* weighing 80–96 g (>2 years old) were purchased from Weihua Toad Farm (Zaoyang, Hubei, China). All experimental procedures adhered to *the NIH Guide for the Care and Use of Laboratory Animals* (8th ed., 2011) and were approved by the Biomedical Ethics Committee of Xi'an Jiaotong University (license number 2016–333). Briefly, toads were housed in a special facility with constant humidity and temperature at 12-h/12-h light/dark cycle and free access to running water and basking area, and were artificially fed mealworms three times per week. Prior to surgery or recording of electrocardiograms (ECGs), the toads were anesthetized by immersion in 0.3% 3-aminobenzoic acid ethyl ester methanesulfonate (MS-222; Cool Seoul Bio, Hefei, Anhui, China) solution buffered to pH 7.7 with sodium bicarbonate, for about 10 min until loss of the eye reflex. To record subepicardial myocyte action potentials (APs), or collect blood sample via heart bleeding, the anesthetized toads were paralyzed by partly destroying brain and spinal cord with a steel probe before exposing the heart. Each toad was finally put to death by isolating the heart after being anesthetized or paralyzed.

Washing of blood in isolated hearts and observing the remaining NRBCs in hearts from healthy toads

Hearts with venous sinus were isolated from five healthy toads. Each heart was immediately placed into a plate (6-cm diameter, 1-cm height) filled with Ringer's solution containing heparin (30 IU mL^{-1}) to let it beat sinusally for 6 min to wash out the blood (see Movie 1). The solution was changed twice during the washing. The washed hearts were fixed with formaldehyde (10%), and embedded in paraffin before being sliced into 5-μm-thick sections. Slices were fluorescence stained to identify remaining NRBCs (not washed out) or were hematoxylin and eosin (H&E) stained to explore the relative position of the NRBCs and the myocardium. Identifying NRBCs was performed using double stainings of Hb and cellular nuclei. Briefly, heart slices were dewaxed by xylene and washed with ethanol (100%, 95%, and 80% in turn) before treating for 10 min in 10 mM sodium citrate at 100°C (to repair the antigen) and for 30 min with 2% bovine serum albumin (BSA) in phosphate buffer saline (PBS) at room temperature (to block non-specific antigens). Then they were incubated overnight in diluent (1:200) of rabbit anti-human Hb antibody (Ab; cat. no. ab191183) at 4°C, for 1 h in diluent (2.5 μg mL^{-1}) of goat anti-rabbit immunoglobulin (IgG) conjugated with Alexa Fluor® 488 (cat. no. ab150077) at 37°C and for 15 min in Hoechst 33,258 (0.5 μg mL^{-1}; Sigma) solution at room temperature. Both Abs were purchased from Abcam (Cambridge, UK) and were diluted with PBS containing BSA (2%). Each incubation was finished by three washes with PBS. Fluorescence microscopic observation and acquiring images were conducted using Nikon NIS-Elements (Nikon Instruments Inc., Tokyo, Japan). H&E-stained slices were observed and images were acquired using Leica Microsystems (Q550CW; Leica Microsystems Inc., Solms, Germany).

Heart needle-injury experiment

The skin of the chest and upper abdomen of 10 anesthetized toads was sterilized with iodine and 75% ethanol. Along the midline, a 1.5-cm-long incision was made to open the upper abdomen. A 25-gauge needle was inserted through the pericardium into the heart apex with 2-mm depth, was kept there for 3 s, and was then drawn out. The abdominal incision was aligned and sutured in layers. Each toad was intramuscularly injected with penicillin G 5×10^4 IU twice daily for two days. On day 3, half of the toads were randomly chosen and hearts were isolated; on day 14, the other half had their hearts isolated. Each heart was treated as described above before being sliced consecutively along the needling route. Sister slices of each heart were respectively H&E stained and Masson trichrome stained to evaluate cardiac injury or recovery and NRBCs in the myocardium.

Transwell assay of effects of cardiac pieces on NRBCs

Preparing NRBCs and cardiac pieces. According to a previous report,[38] from a cut made in the heart apex, 1 mL of blood was collected into 0.5 mL of heparinized Ca^{2+}-free Ringer's solution, then 1.4 mL 32.8% metrizoate solution (Lanospharma Laboratories Co., Ltd, Hong Kong, China) and 0.6 mL 8% ficoll solution (Sigma) were added and centrifuged at 163*g* for 25 min (10°). The cell pellet was further purified by centrifugation until the contamination by leukocytes was below 1% and cell viability was 99%, as determined by microscopy and trypan blue exclusion. About 4×10^8 NRBCs were harvested from 1 mL of whole blood.

Toad hearts were isolated and were washed of blood as above. The ventricles were cut into pieces ($1 \times 1 \times 1$ mm^3) in 70% Leibovitz L-15 medium (Sigma) before use.

5-bromo-2′-deoxyuridine labeling of NRBCs and identifying BrdU-positive cells. NRBCs were incubated in 70% Leibovitz L-15 medium containing 5-bromo-2′-deoxyuridine (BrdU) (5 μg mL^{-1}, Sigma) and FBS (10%) at 25°C for 48 h before use. BrdU-positive cells were identified according to our previous description.[39] Briefly, cells were fixed for 20 min with paraformaldehyde (4%), treated for 30 min with HCl (2 N), incubated overnight with mouse anti-BrdU monoclonal Ab (1:300 dilution; cat. no. b2531, Sigma) and incubated with biotin-conjugated goat anti-mouse IgG (1:1000; cat. no. d110099, Sangon Biotech, Shanghai, China) before incubation for 30 min with Strept Avidin-Biotin complex, staining for 20 min with 3,3′-diaminobenzidine solution and re-staining by hematoxylin.

Transwell assay. Transwell inserts (costar transwelll membranes with 3-μm or 12-μm pores) were placed in 12-well culture dishes to construct the Transwell system. Cardiac pieces were placed in the lower chambers (5 pieces per chamber) and NRBCs with or without BrdU plated in the upper chambers (3×10^5 cells per chamber) and were co-cultured at 25°C in 70% Leibovitz L-15 medium containing FBS (10%), stromal cell-derived factor-1α (100 ng mL^{-1}; Sigma), penicillin G (100 IU mL^{-1}) and streptomycin (100 μg mL^{-1}). Four groups were included: ①NRBCs with BrdU + 3-μm-pore membrane + cardiac pieces ($n = 5$), ②NRBCs with BrdU + 12-μm-pore membrane + cardiac pieces ($n = 5$), ③NRBCs without BrdU + 12-μm-pore membrane ($n = 40$), ④NRBCs without BrdU + 12-μm-pore membrane + cardiac pieces ($n = 40$). On day 3, cardiac pieces in groups ① and ② were sliced and immunohistochemistry-stained for BrdU-positive cells. On days 0, 1, 2, and 3, NRBCs that remained in the upper-side of membranes (not migrated) in groups ③ and ④ were counted ($n = 6$ samples per time point per group) and the cells of day 3 were H&E- and immunofluorescence stained for characterization of phenotypes ($n = 5$ samples per item per group). For immunofluorescence staining, cells were fixed with 4% paraformaldehyde for 20 min and permeabilized with 0.5% Triton X-100 in PBS for 5 min before being treated with 5% BSA blocking solution. Other steps including the diluting of primary and secondary Abs were the same as those described above. Rabbit anti-human myocyte specific enhancer factor 2C (MEF2C) Ab (cat. no. ab227085), mouse anti-synthetic peptide of cardiac troponin T (cTnT) Ab (cat. no. ab33589), and goat

anti-mouse IgG conjugated with Alexa Fluor® 647 (cat. no. ab150115) were purchased from Abcam.

Heart cauterization-injury experiment

Animal model number design. All test items were planned with six samples at each time point. Except for ECG recording, other testing or collection of specimens would injure the heart or cause toad death. Consequently, 48 model-making toads were used for observing heart histological changes after cauterization (days 0, 2, 7, 14, 30, 60, 90, and 120), 18 model toads were used for recording of subepicardial myocyte APs (days 7, 60, and 120), 18 toads were used for evaluation of ventricular contractility (days 7, 60, and 120), and 48 toads were used for biochemical analysis (days 1, 2, 7, 14, 30, 60, 90, and 120). Taking into account the accidental death after surgery, we added a further 38 model-made animals. All told, 170 toads underwent the cauterized heart procedure.

Heart cauterization. Toads were anesthetized and the skin sterilized before a 2.5-cm-long incision in the chest and upper abdomen was made. After cutting off the lower part of the cartilaginous sternum, a small cut was made in the upper part of the pericardium. Through the cut, the heart was exposed. We modified the cautery procedure described by Grivas *et al.*[23] Briefly, at systole, the ventricular apex was cauterized for 2 s twice using a preheated electric soldering iron (flat, oval contact surface: 3 mm long diameter, 2 mm short diameter; 150 watts power). The injured heart was placed back into the pericardial sac followed by dripping penicillin G 3000 IU into the sac and suturing the pericardial incision. Incisions in thoracic and abdominal muscles and skin were sutured hierarchically. Toads were injected intramuscularly with penicillin G for five days, and were provided three days of stagnant water containing gentamycine (2000 IU L^{-1}) for swimming. On planned days, surviving toads were randomly selected to evaluate heart injury and recovery, as follows.

ECG recording and measurement. Lead II ECGs were recorded and analyzed according to Hadji-Azimi *et al.*'s report.[40] Briefly, three needle-electrodes, wired to the ECG module of a physiological signals recorder (Model BL-420F, Taimeng Technology Co., Ltd, Chengdu, China) were respectively inserted into the subcutaneous tissues of two forelimbs and the left hind limb of the toad at anesthesia. For each toad, three successive ECGs were measured to get averages of the QRS complex duration and amplitude and the S-T segment amplitude, respectively. If the Q- or S wave was obscure, it was excluded when measuring the QRS duration and amplitude. And if the S wave was obscure, the voltage at the start of the T wave was regarded as the S-T segment amplitude.

Recording subepicardial myocyte APs. AP recording followed the standard glass-microelectrode technique as described in the literature.[41] Briefly, the toad was paralyzed and the heart exposed. A glass rod was pierced through the connective tissue between venous sinus and bulbus arteriosus to pry up the heart, forcing the apex upward. A silver reference electrode was inserted into the subcutaneous tissue near the heart, and a suspension glass microelectrode was randomly, carefully inserted into a subepicardial myocyte to record APs. If no AP was recorded from 10 different sites within the apical region injured, there was considered to be no virtual CM in the region. The microelectrode was a cone-like glass pipe (about 1 cm length, $\leq$1 mm root diameter, $<$0.5 μm tip diameter) filled with 2.7 M KCl solution and was inserted into a silver wire (100 μm diameter). The tip resistance of the glass-microelectrode was 20–40 M. APs were amplified by an amplifier (Model 8201, Nihon Konden, Tokyo, Japan) and displayed on and printed by a physiological signals recorder (Model RM 6000, Nihon Konden).

Evaluating ventricular contractility. Following the method in the literature,[42] *in vitro* toad heart perfusion and recording ventricular contractility were done. Briefly, from the bulbus arteriosus root, a Straub cannula (8-mm internal diameter) filled with Ringer's solution was inserted into the ventricle. After ligating the bulbus arteriosus root onto the cannula with a cotton thread, the heart with venous sinus was isolated. The Straub cannula was vertically mounted to an iron bracket for constructing an *in vitro* toad heart perfusion system. In this system, the perfusion solution volume/height determines both the preload and afterload of heart pumping. To limit the increase of solution in the venous sinus cavity, the venous sinus was set above the heart body. Through a toad heart clip and a tension transducer (Model FT-100, Taimeng Technology Co., Ltd), the ventricular systole-diastole-curves were recorded with Model BL-420F physiological signals recorder. Ringer's solution was gradually added into the Straub cannula to induce the maximal heart systole and diastole. The optimal solution height and the maximum ventricular tension together indicate the ventricular contractility.

Heart histology. Sister sections of each heart were respectively H&E- and Masson trichrome stained. Myocardial injury and recovery and NRBC infiltration were examined microscopically. Quantifying collagen fibrils was conducted using Leica Microsystems.

Biochemical analysis. Toad serums were separated from the blood samples using a routine method and were stored at −20°C. Heart apex samples were stored at −80°C before being thawed, cut into pieces, and lysed in lysis buffer (50 mM Tris-HCL, pH 7.5, 150 mM NaCL, 2 mM EDTA, 1% NP40, 1% TritonX-100) containing a protease inhibitor cocktail and homogenized on ice. The homogenate was centrifugated at 3000*g* at 4 °C to obtain total protein. The Bradford method was used to measure protein concentrations. Analysis of cytokines and enzymes used enzyme-linked immunosorbent assay (ELISA) or Western blotting.

ELISA. ELISA was performed according to the kit manufacturers' instructions and as described in the literature.[43] Briefly, a 96-well plate was coated with detection Reagent A

for 12 h at 4°C. Then, 50 μL of serum sample or total protein extracted from the cardiac tissue sample was added into the 96-well plate, which had been coated with the specific Ab for each cytokine or enzyme, and detected via the ELISA sandwich technique. ELISA kits for tumor necrosis factor-α (TNF-α, cat. no. tw043962), interleukin (IL)1β (cat. no. tw043835), IL6 (cat. no. tw043836), IL11 (cat. no. tw044182), and vascular endothelial growth factor (VEGF, cat. no. tw044059) were purchased from Shanghai Tongwei Industrial Co., Ltd (Shanghai, China), and kits for erythropoietin (EPO, cat. no. M25016752) and cardiotrophin-1 (CT-1, cat. no. E08454h) were from Cusabio Biotech Co., Ltd (Wuhan, Hubei, China).

Western blotting. Western blotting assay was done according to our previous report.[39] Briefly, protein samples (40 μg) were separated by electrophoresis in 7.5% polyacrylamide-SDS gel and electrophoretically transferred to a nitrocellulose membrane of 0.45-μm pore size in glycine-methanol buffer. The membrane was blocked in Odyssey Blocking Buffer (LI-COR Biosciences, Lincoln, NE, USA), then incubated overnight at 4°C in rabbit anti-human matrix metalloproteinase 2 (MMP2) Ab diluent (1:1000; cat. no. 4022, Cell Signaling Technology, Danvers, MA, USA) or in rabbit anti-human MMP9 Ab diluent (1:1000; cat. no. 2270, Cell Signaling Technology), and finally incubated in IR Dye 800CW-goat anti-rabbit IgG (1:10,000; cat. no. 926–32211, LI-COR Biosciences). Bands were visualized with Odyssey Imager and quantified with NIH Image J software. Equal protein loading was checked by detection of glyceraldehyde-3-phosphate dehydrogenase using rabbit anti-human glyceraldehyde-3-phosphate dehydrogenase Ab (1:3000; cat. no. 2118, Cell Signaling Technology).

Effect of CT-1 on NRBCs

Exploring the effect of CT-1 on NRBC, migration was performed using a Transwell assay. NRBCs were plated in the upper chamber (12.0-μm-pore Transwell membrane). Recombinant human CT-1 (hCT-1, 0.5 nM, ProSpec, Rehovot, Israel) was added into the medium. After a 72-h culture, NRBCs remaining on the upper side of the membrane were counted.

To investigate the effect of CT-1 on NRBC phenotypes and the influence of the local environment on the effect, pure NRBCs that were suspended in 70% Leibovitz L-15 medium containing FBS (10%) and whole blood that was diluted (100-fold) by serum were respectively placed into 6-well plates (2×10^7 cells per well) and cultured in the presence or absence of hCT-1 (0.5 nM) for seven days at 25°C. Cell vegetal status was observed every day. Cells of three days- and seven days culture were H&E-stained, or lysed to analyze Hb, MEF2C, cTnT, and tropomyosin by Western blotting. Mouse anti-chicken tropomyosin Ab (cat. no. T9283) was purchased from Sigma. IR Dye 800CW-goat anti-mouse IgG (1:10,000; cat. no. bs-40296G-IRDye8) was from LI-COR Biosciences. Other primary and secondary Abs were the same as above. Primary Abs were used at 1:1000–1:5000 dilution.

Statistics

Three to six samples were tested for each group, taking into account homogeneity of test values and frugality, and elimination of substandard samples (contaminated samples, samples with the background of pericardium-heart adhesion). For microscope cell counting, cells in three high power fields randomly chosen were totaled as one sample data. For ELISA, each sample underwent three tests for an average result. Data were presented as mean ± SD for at least three samples per group. The statistical significance of differences between two groups was determined using unpaired Student's *t*-test, and differences among multiple groups were determined using one-way analysis of variance (ANOVA) followed by Dunnett's *post hoc* test. Values of $P < 0.05$ (two-tailed) were considered significant. All statistical analyses were performed using GraphPad Prism v5.0 software (La Jolla, CA, USA).

Results

NRBC infiltration into myocardium was seen in the healthy toad hearts

Under the microscope, the layout of toad ventricular muscles appeared spongy. The trabecular spaces were connected to each other forming the ventricular chamber. The ventricular wall was non-uniform in thickness. The thinnest part of the apical wall was 40–90 μm (including the epicardium). There were blood vessels in the epicardium but not in the myocardium and endocardium. Although each heart had been washed of blood, a few NRBCs were not washed out. Some of them were free in the trabecular spaces, some others adhered to the endocardium, and the rest entered the myocardium (overlapping with the muscle bundles completely or partly) (Figure 1), indicating NRBC infiltration into the myocardium. The infiltrated (entering the myocardium completely) and infiltrating (entering partly) NRBCs in healthy toad hearts were sparse, and the distribution was inhomogeneous, averaging 6.3 ± 1.2 NRBCs per mm^2 of cardiac tissue (mean ± SD, $n = 5$).

NRBC infiltration increased during the recovery of myocardial needle-injury

The myocardial needle-injury recovered within two weeks. As shown in Figure 2, there was no scar in the recovery area. The density of collagen fibers in the recovery area was similar to that in the surrounding area. Besides inflammatory response at the early stage, NRBC infiltration into myocardium increased during the recovery.

Cardiac pieces induced NRBC infiltration and transition toward CM

In the transwell co-culture system, NRBCs did not pass through the 3-μm pore membrane, but passed through the 12-μm pore membrane and infiltrated into the cardiac pieces (Figure 3(a) and (b)). The number of NRBCs in the upper chamber decreased daily, and the decrease in numbers of the group with cardiac pieces was more significant

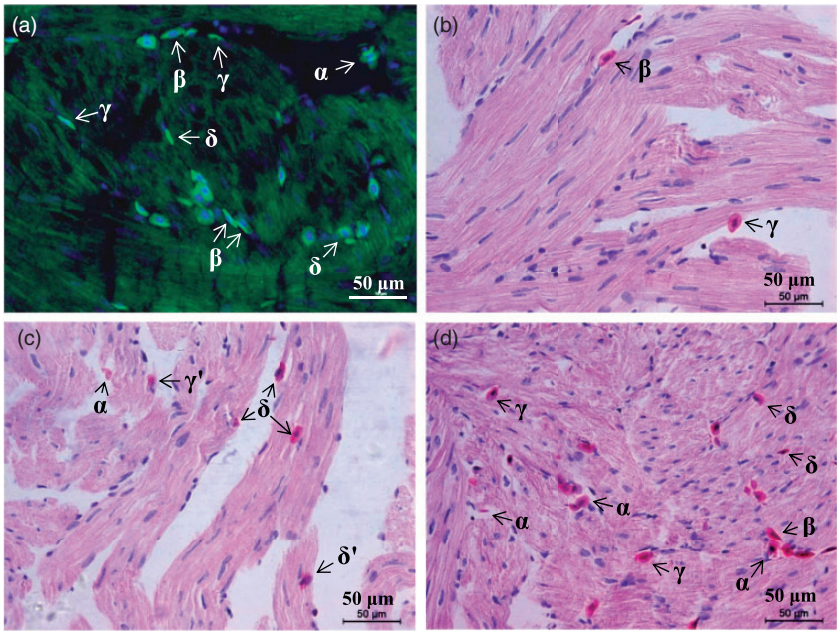

Figure 1. There are infiltrated and infiltrating nucleated red blood cells (NRBCs) in the myocardium of healthy toads. Hearts ($n = 5$) isolated were washed of blood. Heart slices were fluorescence stained (a) or hematoxylin and eosin (H&E) stained (b)–(d). (a). NRBCs were identified by hemoglobin (green) and the nucleus (blue). (b)–(d). Representative fields in which longitudinal (b) and (c) and oblique (d) muscle bundles were included, and NRBCs were in different positions or states: some were free in the trabecular spaces (ventricular chamber) (α), some others adhered to the endocardium (β), and the rest had been entering the myocardium (overlapped partly (γ and γ') or completely (δ and δ') with the muscle bundles, including NRBC in the upper, muscle bundle in the lower (γ and δ) and vice versa (γ' and δ')). (A color version of this figure is available in the online journal.)

than those of the group without cardiac pieces ($P < 0.05$ or 0.01) (Figure 3(c)). At day 3, NRBCs of the group with cardiac pieces, compared with those of the group without cardiac pieces, became less sensitive to eosin (Figure 3(d) and (e)) although were still positive for expression of Hb (Figure 3(f) and (g)), and became positive for expressing cTnT and MEF2C, two special markers for CMs (Figure 3(f) to (i)).

Complete regeneration followed severe myocardial damage

After heart apex cautery, 81.2% toads (138 in 170) survived to the planned dates of the experiment. As shown in Figure 4, Figures S1 and S2, Online Movies 2 and 3, and Tables S1 and S2, approximately 5% of the ventricle was injured to varying degrees: the apical shallow tissues were severely damaged and the deep tissues were moderately to mildly injured. The maximum lesion depth and width were 0.5 mm and 2.5 mm, respectively. The nucleus of injured cells disappeared, shrank, or lowered sensitivity to hematoxylin. The lead II ECG's P-R interval of normal toads was relatively long, and the T wave was downward, opposite to the polarity of the QRS wave. ECGs of heart-cauterized toads became abnormal: the QRS complex's duration shortened and amplitude lowered, while the S-T segment lifted. No subepicardial myocyte AP was recorded in the cauterized region. The ventricular contractility of the injured hearts decreased significantly. Most of the hearts underwent inflammation, scarring, vascularity, and myocardial regeneration beginning in the deep area and extending to the shallow area, and gradually recovered. On day 120 after cauterization (dac), the hearts' ECGs normalized, hearts' exterior appeared normal, the ventricular contractility normalized, and subepicardial myocyte APs could be recorded; scar and new blood vessels disappeared, replaced by new myocardium. Pericardium-heart adhesion occurred in a few toads (19 in 138), delaying myocardial regeneration. These toads were found at different time points and were eliminated from the experiment. Microscopically, the adhesion looks like epicardial thickening or pericardial invasion. Pericardium tightly wrapping around heart due to surgery might cause the adhesion.

NRBC infiltration increased throughout myocardial regeneration and NRBCs were seen in the neomyocardium

Numbers of NRBCs (not washed out) in 0–120 dac of hearts were more than that in normal hearts (Figure 5). Early at 10 min (0 dac), NRBCs as well as inflammatory cells gathered into the shallow area, and in the deep areas NRBC infiltration began to increase (Figure 5(b)). The shallow area underwent inflammation, scarring, and vascularity before NRBC infiltration and myocardial regeneration began. The scarring lasted about 30 days and then the scar gradually vanished (Figure 6). As shown in Figure 7, the extravascular NRBCs are infiltrated NRBCs. Notably, new myocardial tissues that appeared in both the deep areas (Figure 5(c)) and the shallow area (Figure 7(a) and (e)) were more sensitive to eosin than mature myocardium but less sensitive than NRBCs, and there were NRBCs in the newly formed myocardium (Figure 7(f)).

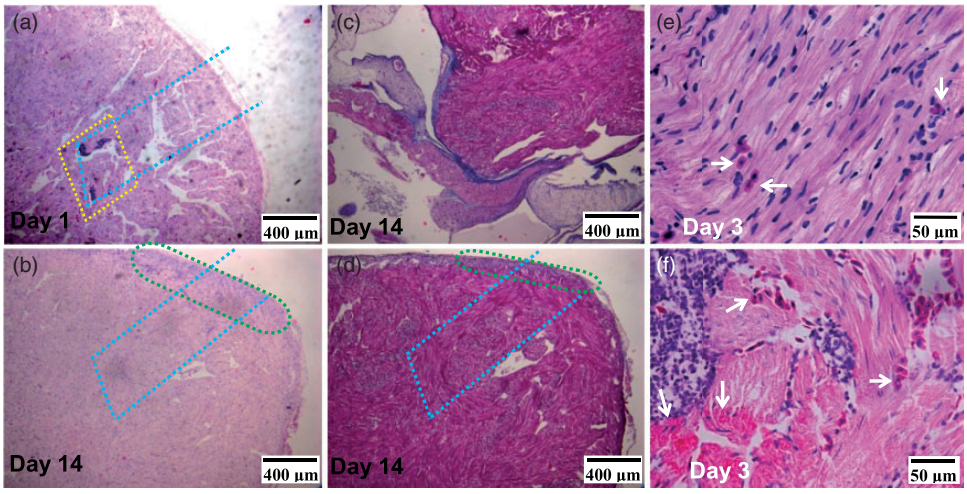

Figure 2. Representative slices of toad hearts after needling-injury. Slices were H&E stained (a), (b), (e), and (f) or Masson trichrome stained (c) and (d). Inflammatory focus indicating injury (ringed by the yellow dot-line) was clear at day 1 (a) and recovered at day 14 (b). Inflammatory residual (ringed by the green dot-line) (b) and (d) indicates the range of needling entrance. Delineated by the blue dot-line (a), (b), and (d) is a simulated needling track. (b) and (d) are from two sister slides of the same heart. (c) and (d) are from the same slide. (c). Tissues near the bulbus arteriosus root showing positively stained collagen fibers (blue) and muscle fibers (magenta). (d). Tissues near the apex. (e) and (f) are from the same slide. (e). Uninjured area. (f). Injured area. Infiltrated and infiltrating NRBCs (white arrows) in injured area were more than those in uninjured area. (A color version of this figure is available in the online journal.)

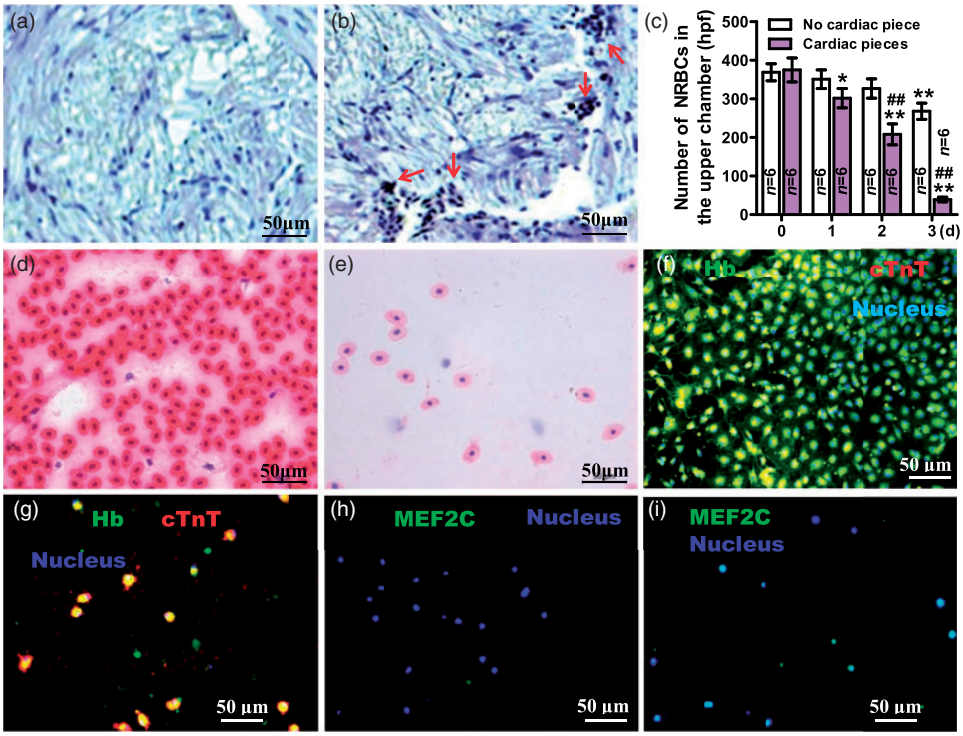

Figure 3. Transwell assay of effects of cardiac pieces on NRBCs. NRBCs with (a) and (b) or without (c)–(i) 5-bromo-2′-deoxyuridine (BrdU) were plated in the upper chamber and cardiac pieces placed (a), (b), (e), (g), and (i) or not (d), (f) and (h) in the lower chambers. Transwell membranes were 3-μm pore-size (a) or 12-μm pore-size (b)–(i). (a) and (b). Slices of cardiac pieces at day 3 were immunohistochemistry stained for NRBCs with BrdU. There were NRBCs with BrdU (tan-colored nuclei, red arrows indicated) in (b) but not in (a). (c). Statistics on the number of NRBCs in the upper chamber. From each chamber, three high power fields (hpf) were randomly chosen for cell counting and totaling. Data were presented as mean ± SD, $^{*}P < 0.05$ and $^{**}P < 0.01$ (two-tailed) vs. 0 day (d) were calculated by one-way analysis of variance (ANOVA) followed by Dunnett's *post hoc* test; $^{\#\#}P < 0.01$ (two-tailed) vs. no cardiac piece were calculated by unpaired Student's *t*-test. In the presence of cardiac pieces, NRBCs became less sensitive to eosin, and became positive for expressing cardiac troponin T (cTnT) and myocyte specific enhancer factor 2C (MEF2C) besides hemoglobin (Hb). (d) and (e). H&E-stained NRBCs at day 3. (f)–(i). Fluorescence-stained NRBCs at day 3. (A color version of this figure is available in the online journal.)

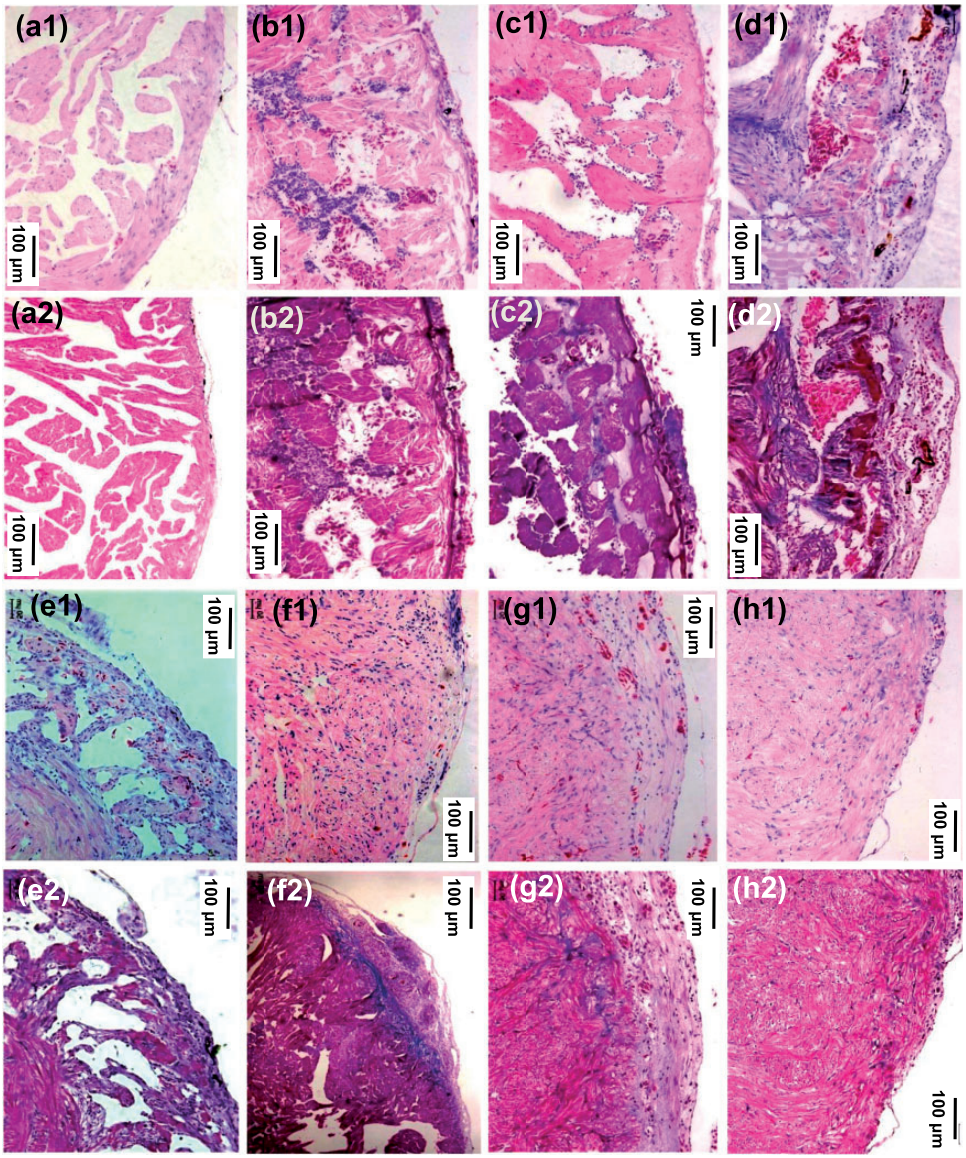

Figure 4. Representative slices of toad hearts after cautery-injury. Sister slices of each heart were respectively H&E stained (a1)–(h1)) and Masson stained (a2)–(h2) ($n = 4$, respectively). (a1) and (a2). Control (normal). (b1) and (b2). On day 0 (ten minutes) after cauterization. (c1)–(h1) and (c2)–(h2). On days 7, 14, 30, 60, 90, and 120 after cauterization. (A color version of this figure is available in the online journal.)

Multiple mediators were involved in myocardial regeneration

TNF-α and IL1β levels in the injured cardiac tissue increased quickly but briefly, both peaked at 1 dac and dropped to nearly normal at 7 dac (Figure 8(a) and (b)). IL6 level in the injured cardiac tissue increased within the first week and peaked at 1 dac (Figure 8(c)). IL11 levels in cardiac tissues of 2–30 dac and in serums of 2–60 dac were elevated (Figure 8(d) and (e)). CT-1 levels in serums and cardiac tissues of 2–90 dac continued to rise and peaked at 30 dac (Figure 8(f) and (9)). EPO level in serums of 2–60 dac was increased (Figure 8(h)), but no EPO was detected in cardiac tissues. VEGF levels in cardiac tissues of 2–60 dac and in serums of 7–30 dac increased, and both peaked at 14 dac (Figure 8(i) and (j)). Cardiac tissue MMP2 continued to rise from 2 to 90 dac and cardiac MMP9 increased from 2 to 60 dac, and both peaked at 14 dac (Figure 8(k) and (l)).

CT-1 induced NRBC transition toward CM

As shown in Figure 9, hCT-1 (0.5 nM) treatment altered the phenotype and fate of NRBCs: their sensitivity to eosin lowered and Hb protein decreased, while cTnT, MEF2C, and tropomyosin (a myocyte marker) increased in three-days of culture; some of the cells died on day 4 and no living cells were seen on day 7. But hCT-1 at 0.5 nM did not influence NRBCs in whole blood (diluted by toad serum). The transwell assay showed that hCT-1 (0.5 nM) did not induce NRBCs to migrate in three days (Figure S3).

Discussion

The study found the following: NRBC infiltration into myocardium occurred in healthy toad hearts; toad hearts could recover scarlessly from myocardial injury, NRBC infiltration increased during the recovery and there were NRBCs

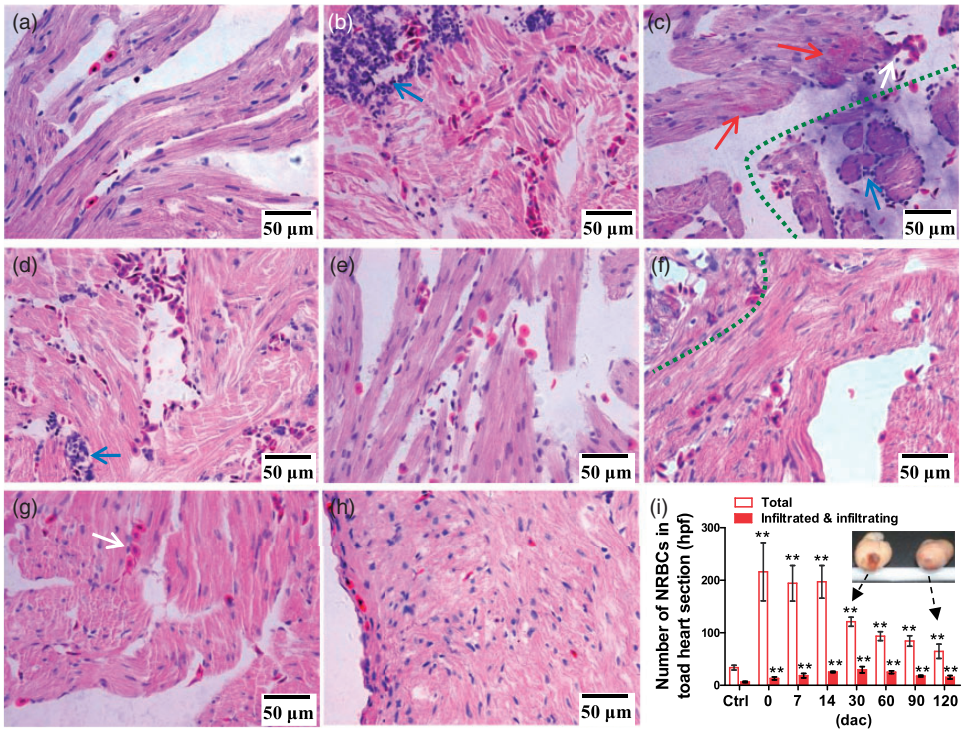

Figure 5. NRBCs in toad hearts. (a)–(h). H&E-stained heart slices (high power fields). (a). Normal heart slice. There is no blood vessel in the myocardium. (b)–(h). Slices of hearts at 0, 7, 14, 30, 60, 90, and 120 dac (days after cauterization), respectively. The severely damaged area (shallow area) and the mildly injured area (deep area) are divided by a green dashed curve (c) and (f). Blue arrow, inflammatory cells; white arrow, NRBC cluster; red arrow, new myocardium. (i). Statistics on NRBCs. In each section, three high power fields were randomly chosen for cell counting and totaling. Data are presented as mean ± SD, $n = 4$, respectively; $^{**}P < 0.01$ (two-tailed) vs. control (ctrl) group was calculated by Dunnett's *post hoc* test after ANOVA. (A color version of this figure is available in the online journal.)

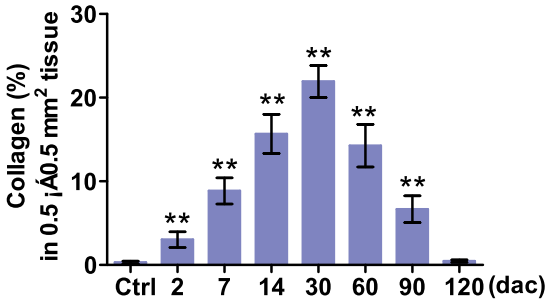

Figure 6. Collagen fibrils in toad hearts at indicated days after cautery-injury. Heart slices were Masson stained. Quantifying collagen fibrils used Leica Microsystems. Data are presented as mean ± SD, $n = 4$, respectively; $^{**}P < 0.01$ (two-tailed) vs. ctrl group was calculated by Dunnett's *post hoc* test after ANOVA. (A color version of this figure is available in the online journal.)

in the newly formed myocardium; myocardial injury induced NRBC infiltration and transition toward CMs. Taken together, the results suggest that, at least in the toad, the NRBC is a cell source for CM renewal/regeneration.

There is a consensus that the adult heart has regenerative potential. Ectotherms are generally more capable of regenerating CMs than mammals.[2] Within the same species, heart regeneration is more obvious in the case of systemic hypoxia than in the case of non-hypoxia.[2,8] However, the source of the new CMs is still uncertain. Although a few CMs within the adult heart have been found to re-enter the cell-cycle,[7–9] it does not directly mean proliferation. To observe the CM-reentry of cell cycle, cell lineage tracing technique was used. However, this technique usage is unable to identify new CMs from existing CMs. So, it is questionable to attribute the CM regeneration fully to proliferation of existing CMs, whether in mammals or ectotherms.

Given that the first CM originated from the embryonic stem cell,[12] adult stem/progenitor cells are attracting attention, and have been investigated for almost twenty years for their roles in CM regeneration.[15] Among the somatic stem/progenitor cells studied, skeletal myoblasts are unable to transdifferentiate into CMs;[44] adipose-derived stem/progenitor cells usage in infarct heart reduces scar formation and improves perfusion and thus improves cardiac function, but does not lead to direct differentiation into CMs;[44] cardiac stem/progenitor cells may differentiate into CMs, but it is not easy to collect sufficient numbers of these cell types and their efficiency is usually low.[16,45] BM resident stem/progenitor cells are relatively easy to obtain, which is conducive to autologous transplantation for cell therapy. Because a few BM stem/progenitor cells can enter circulating blood, it does not rule out that some somatic stem cells including cardiac stem/progenitor cells are derived from BM stem/progenitor cells, and the BM stem/progenitor cell-based cell therapy is also to explore, using a pharmacological approach, whether and how the circulating BM resident stem/progenitor cells participate in myocardial regeneration. In practice, BM mononuclear cells

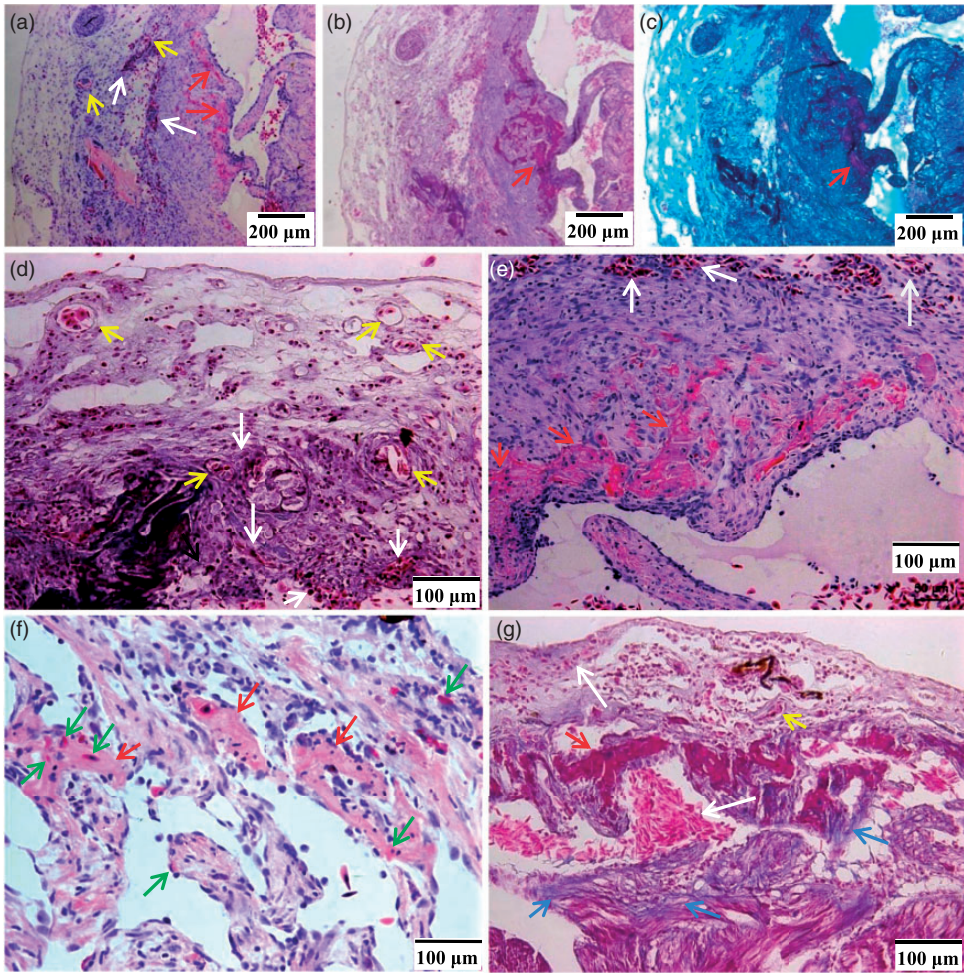

Figure 7. Representative photographs showing neovascularity, NRBC infiltration and new myocardium formation in toad hearts at 30 dac. Heart slices were H&E stained (a) and (d)–(f) or Masson stained (b), (c), and (g). For Masson staining, muscle fibers were colored purple by ponceau S-acid Fuchsin, collagen fibrils were colored blue (blue arrows) by aniline blue (b) and (g) or colored cyan by light green (c). (a)–(c). Low power fields. (d)–(g). High power fields. (a)–(e) and (g) were from sister slices of the same heart, and (d) and (e) from the same slice. The severely damaged area underwent inflammation, scarring, and vascularity (yellow arrows) before NRBC infiltration began. The extravascular NRBCs (white arrows) were infiltrated NRBCs. New myocardium (red arrows) gradually formed from the deep area to the shallow area (a)–(c), (e), and (g)); the neomyocardium was more sensitive to eosin than mature myocardium but less sensitive than NRBCs (a), (e), and (f), and were more sensitive to ponceau S-acid Fuchsin than NRBCs (b) and (g). There were NRBCs (green arrows) in the newly formed myocardium (f). (A color version of this figure is available in the online journal.)

(BMMNCs) were the first to be isolated or directly applied. BMMNCs are a heterogeneous population which includes a small number of hematopoietic stem cells (HSCs), endothelial progenitor cells (EPCs), and mesenchymal stromal/stem cells (MSCs), whereas the major proportion comprises cells of the hematopoietic lineage at various maturation stages,[46] but not including orthochromatic normablasts. In the process of isolating BMMNCs, there is a step to eliminate RBCs.[39] Orthochromatic normablasts as well as mature RBCs and even some polychromatophilic normablasts will be lysed by the RBC lysis buffer.[39] Some research groups have studied the effects of BMMNCs as a mixture on myocardial regeneration, while others have investigated the purified cells of specific cell types.[47] For BMMNCs, different groups have reported contradictory results.[48] In other words, it is still unknown whether transplantation of the BMMNC mixture is beneficial for CM regeneration.[15] Concerning MSCs, it is believed that these cells may contribute to myocardial regeneration through paracrine, immunomodulation, and an involvement in angiogenesis.[44,48] For example, the involvement of EPCs in angiogenesis is MSCs-dependent.[49] Also, MSCs in medium containing CT-1 and 5-azacytidine may differentiate into CM-like cells.[13] EPCs as a pro-vasculogenic subpopulation of HSCs are involved in angiogenesis, and through paracrine to benefit myocardial regeneration.[50] Meanwhile, the adult mouse heart snRNA-seq has revealed a cell population that comprises endothelial markers as well as markers clearly related to CM function.[12] Whether EPCs are a source of the CM should be further investigated. C-kit$^+$ HSCs have prominent cardiac recovery after acute myocardial infarction,[51] and in CM differentiation medium can differentiate toward CMs and secrete a variety of cytokines and growth factors.[16,17] In summary, among BM resident stem/progenitor cells, c-kit$^+$ cells seems to be the most well-defined CM-differentiated subpopulation, but the efficiency is low

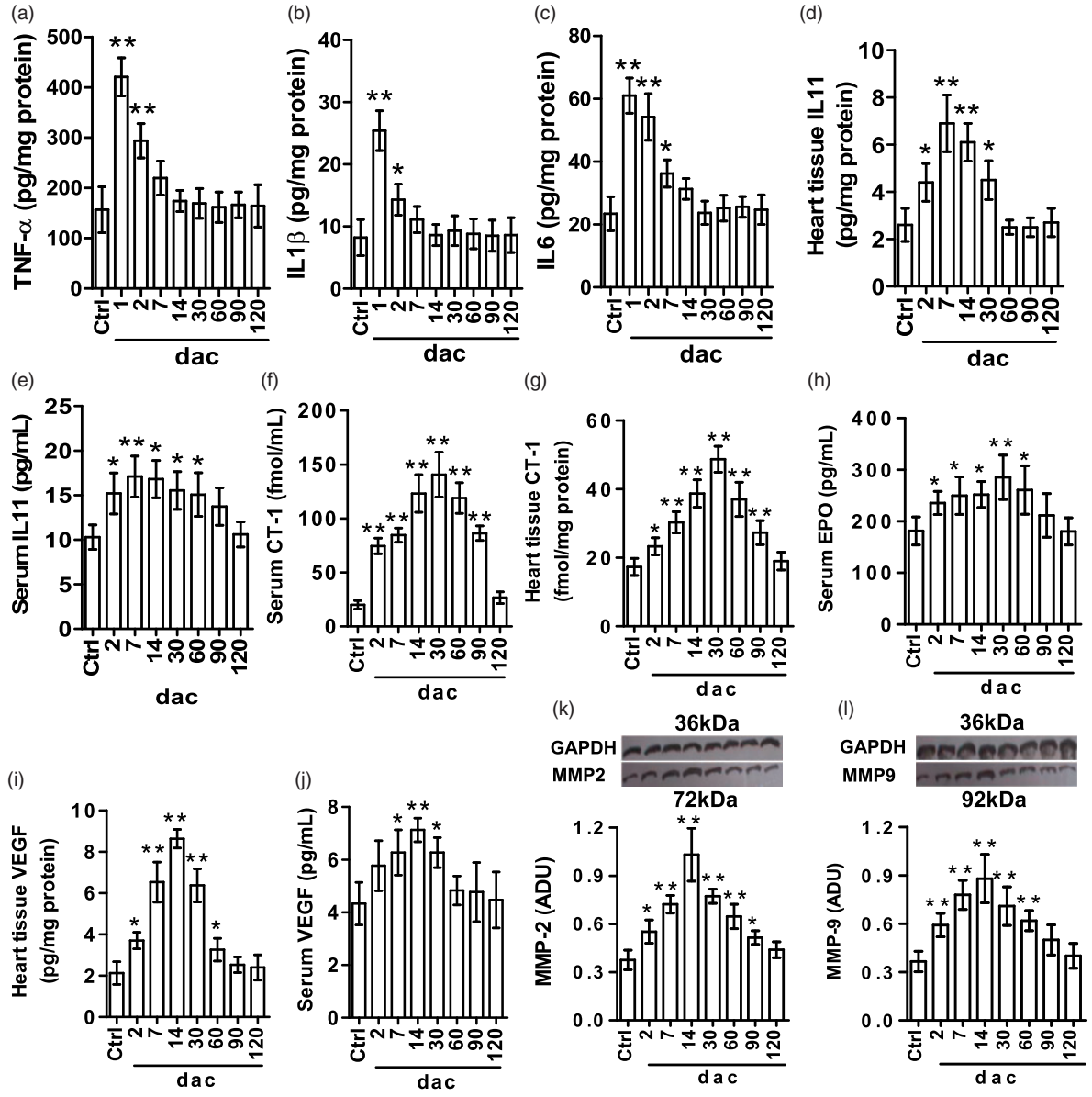

Figure 8. Biochemical assay results. At indicated days after cautery-injury (dac), samples of blood and/or the apical tissue were collected to analyze relevant substances by enzyme-linked immunosorbent assay or Western blotting. Data are presented as mean ± SD, $n = 3$, respectively; $^{*}P < 0.05$ and $^{**}P < 0.01$ vs. Ctrl group were calculated by Dunnett's *post hoc* test after ANOVA. (a). Apical TNF-α. (b). Apical IL1β. (c). Apical IL6. (d). Apical IL11. (e). Serum IL11. (f). Serum cardiotrophin-1 (CT-1). (g). Apical CT-1. (h). Serum erythropoietin (EPO). (i). Apical vascular endothelial growth factor (VEGF). (j). Serum VEGF. (k). Apical matrix metalloproteinase 2 (MMP2). (l). Apical MMP9. ADU: arbitrary densitometric unit relative to glyceraldehyde-3-phosphate dehydrogenase (GAPDH).

due to their multipotent differentiation potential (CMs, smooth muscle cells, and endothelial cells)[52] and poor survival and maintenance in the damaged heart tissue.[16,17]

NRBCs are BM resident immature RBCs. Mammalian circulating NRBCs are very rare, which is not conducive to explore the role of NRBC in CM renewal/regeneration. Lower vertebrates including amphibians are rich in circulating NRBCs. Here we find toad NRBCs transdifferentiation to CMs. This finding is not necessarily simply transferable to humans, but it is instructive. At least we can infer that lack of NRBCs is a possible reason for the limited human heart regeneration. No doubt, ectotherms' abundant circulating NRBCs is related to the low blood partial pressure of O_2 due to the slow body metabolism.[2,53] For humans, the hypoxic microenvironment of infarcted myocardial tissue may also be suitable for NRBCs to survive and transdifferentiate into CMs.

In this study, the washing out of blood in hearts was a research technique. A few NRBCs were not washed out. The free NRBCs in the trabecular spaces can be used as a reference standard for identifying NRBCs in the myocardium. Some of the adherences of NRBCs to the endocardium were real, the others might be caused by the washing. However, the washing could not cause NRBCs to enter the myocardium from trabecular spaces because NRBCs were large in size (15.5–21.9 μm long diameter, 10.3–14.2 μm short diameter) and the endocardial barrier was not easily damaged by Ringer's solution in 6 min at <1 cm-height of perfusion pressure (see Online Movie 1). The conclusion is that the myocardial NRBCs were present

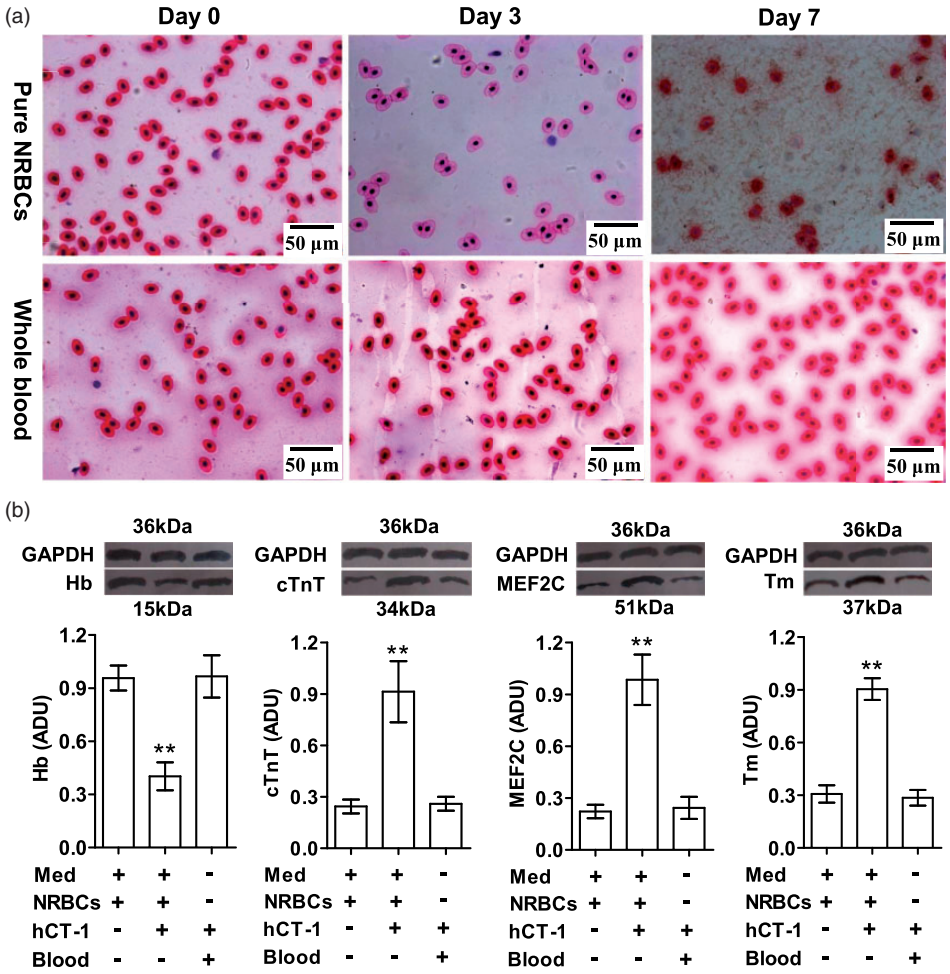

Figure 9. Effects of CT-1 on NRBCs. Toad pure NRBCs and whole blood cells were treated for seven days by hCT-1 (0.5 nM) in 70% Leibovitz L-15 medium (Med, for pure NRBCs) or in toad serum (for whole blood cells). (a). H&E-stained cells. (b). Western blotting assay of Hb, cTnT, MEF2C, and tropomyosin (Tm) proteins in the homogenates of cells on day 3. Data are presented as mean ± SD, $n = 3$, respectively; $^{**}P < 0.01$ (two-tailed) vs. Med (+) + NRBCs (+) + hCT-1 (−) + Blood (−) was calculated by Dunnett's *post hoc* test after ANOVA. (A color version of this figure is available in the online journal.)

there before the heart was isolated. Anuran amphibian hearts have been denied hematopoietic activities.[54] Therefore, the NRBCs that overlapped completely with muscle bundles were infiltrated NRBCs, and the NRBCs that overlapped partly with muscle bundles were infiltrating NRBCs. NRBCs adhering to the endocardium might be the first step for infiltrating into the myocardium. In the healthy toad heart, the distribution of infiltrated and infiltrating NRBCs was sparse and inhomogenous (Figure 1).

To our knowledge, this is the first time to find, in healthy vertebrates, NRBC infiltration into the myocardium, and the first time to find the appearance of RBCs in tissue other than blood and hematopoietic tissues, implying a physiological phenomenon. Previously, it was believed that RBCs leaving the blood signified a disease, for example, angiorrhexis, serious vascular leakage, or drug poisonings.

Carbon-14 dating has revealed that nearly half of CMs are exchanged during the human life span,[5,6] suggesting physiological CM renewal. It can be imagined that in a healthy heart, a few CMs may die from aging, mutation, or other causes (occasional emergency or stress), which need replenishment. Intraventricular injection is a common clinical practice. The needle-injury to the myocardium is tiny and thus is usually ignored. Here we used it as an enlarged model of physiological CM-loss. The result suggests that NRBC infiltration was related to physiological CM renewal.

Our needling- and transwell experiments proved that myocardial injury or CM loss induced NRBC infiltration. The transwell experiment also showed that in a myocardial injury-based condition, NRBCs transdifferentiated toward CMs. In the transwell system, the migrated NRBCs had three places to go: attaching to the underside of the transwell membrane, infiltrating into the cardiac pieces, or falling onto the lower chamber bottom. It was difficult to directly count NRBCs that infiltrated into the cardiac pieces and observe their phenotypes. Cells on the lower chamber bottom included other cell types from the cardiac pieces. So the unmigrated NRBCs were counted and characterized to indirectly reflect NRBC migration and transition toward CM. BrdU-labeled NRBCs were also used to directly verify the NRBC infiltration.

To verify NRBCs participating in myocardial regeneration, we performed the heart-cautery experiment. Cautery severely damaged the shallow apical tissues and just

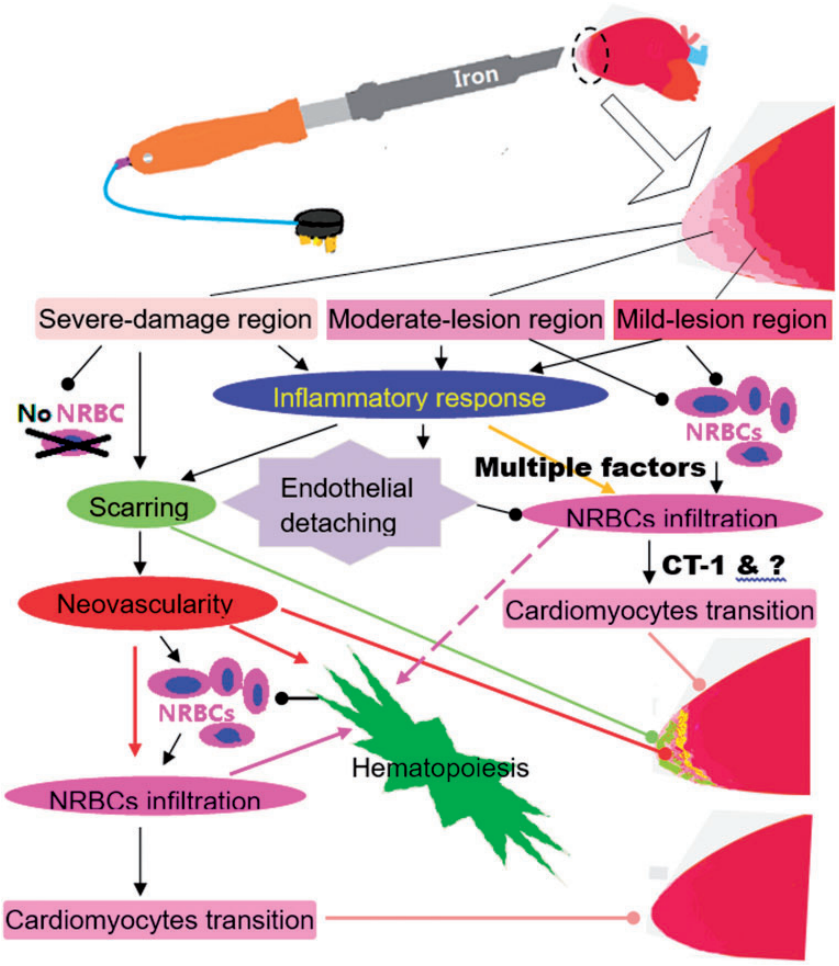

Figure 10. Schematic illustration of the toad heart regeneration after cauterization. The apical tissues were injured to varying degrees, inflammatory response quickly followed. The inflammation induced endothelial cells detaching from the endocardium, facilitating NRBC infiltration. NRBC infiltration and transition to cardiomyocyte soon began in the mild-to-moderate injury regions. The disruption of trabecular spaces caused a cessation of NRBC supply in the severely damaged region, so the region had to undergo chronic inflammation, scarring, and neovascularity before NRBC infiltration began. The demand for NRBCs activated systemic hematopoiesis. Multiple factors (cytokines, growth factors, enzymes, hormones, etc.) directly or indirectly contributed to NRBC infiltration and transition to cardiomyocyte. (A color version of this figure is available in the online journal.)

moderately or slightly injured the deep myocardium. NRBC infiltration increased directly in the deep areas. Because of the tissue damage and the pause of NRBC supply through trabecular spaces, the shallow area underwent chronic inflammation, scarring, and vascularity before NRBC infiltration, delaying myocardial regeneration. So the whole regeneration took four months. As illustrated in Figure 10, the CM regeneration depended on the NRBC infiltration. The increased NRBC infiltration throughout myocardial regeneration and the appearance of NRBCs in the newly formed myocardium (Figure 7(f)) support NRBCs participating in myocardial regeneration, suggesting NRBCs as a cellular source of new CMs.

According to this finding, all fish, amphibians, reptiles, and birds should possess high cardiac regenerative capacities because they have sufficient NRBCs. In fact, most of the fish and amphibians studied showed a remarkable ability to regenerate heart.[1,21,23,24,55,56] However, medaka (*Oryzias latipes*), a fish species, and *Xenopus laevis*, a frog species, have been reported respectively by Ito *et al.*[57] and Marshall *et al.*[58] to lack the ability. In particular, Mexican tetra (*Astyanax mexicanus*) subpopulations surface fish and Pachón cavefish share sufficient genetic similarity. Stockdale *et al*. recently reported that surface fish completely regenerated their ventricular apex after resection, while Pachón cavefish formed permanent fibrotic scars.[59]

Multiple elements may influence the process of myocardial regeneration and the judgment of results. The first one is the operation procedure and technique. Adhesion or/and blood clot may cause chronic inflammation and scarring, delaying myocardial regeneration. In our experiment, the pericardial incision was made far away from the apex to avoid postoperative adhesion, and the ventricular apex was cauterized at systole to minimize bleeding. In Marshall *et al*.'s study, apical resection was performed at diastole.[58] According to their Figures 1(e), 2(d), 8, and Supplemental File 1, the large blood clot due to bleeding and the postoperative adhesion due to no suture of the pericardial incision had influenced the myocardial regeneration. The second element is the injury model and degree of lesion. This determines the recovery time and pattern and the end time of the experiment. The third one is the

misjudgment. Both Ito *et al*. and Marshall *et al*.'s studies used an apical resection model. Some of the "un-regenerative hearts" they presented actually possessed a new, perfect apex without collagen; and the collagen-positive tissue they showed was small and was far from the new apex. Refer to Figure 1(m) in Ito *et al*.'s article,[57] and Figures 2 (d) and 8 in Marshall *et al*.'s article.[58] As for Stockdale *et al*.'s data for the Pachón cavefish, it seems that the scar size at day 100 after apical amputation is significantly smaller than that at day 21, suggesting significant reduction of scar from day 21 to day 100. Refer to their Figure 1(d) and (f).[59] Other elements such as animal species, strain, age, metabolic state also affect the myocardial regeneration. For example, comparing the sizes of scars in Figure 1(d) to (f) presented in Stockdale *et al*.'s article,[59] it seemingly can conclude that neomyocardium formation and scar disappearance in the heart of Pachón cavefish are much slower than that in surface fish.

NRBC infiltration and transition to CM involve a series of biological processes. A zebrafish study revealed that cardiac injury was followed by inflammation and endothelial cells detaching from the myocardium,[60] facilitating NRBC infiltration. The demand for NRBCs may activate systemic erythropoiesis. Infiltration of NRBCs into the scar tissue requires vascularity. Neovascularity involves growth factors.

TNF-α and IL1β are pro-inflammatory cytokines. IL6, IL11, and CT-1 are glycoprotein130 utilizing cytokines. Glycoprotein 130 signals are involved in neovascularity, hematopoiesis, and myocardium development.[61,62] IL-6 has pro- and anti-inflammatory effects[63] and plays a role in fibrosis.[64] IL11 is involved in cardiac fibrosis,[65] recruitment of endothelial cells, and hematopoiesis.[66] Many factors including myocardial infarction stimulate CT-1 release from the myocardium, endothelium, and adipose tissue.[67] It has been reported that CT-1 induces embryonic stem cells and MSCs to differentiate toward CMs.[13,68] EPO is a key hormone for erythropoiesis. VEGF is key for angiogenesis.[69] MMP2 plus MMP9 degrades type IV collagen and laminin-5 in the basement membrane, which is an essential step for cell metastasis.[70,71] MMP2 and MMP9 also promote VEGF mobilizing endothelial cells.[71,72] Our results suggest that TNF-α, IL1β, IL6, IL11, EPO, VEGF, MMP2, and MMP9 are involved in NRBC infiltration into the myocardium.

Since CT-1 secretion increased throughout the myocardial regeneration, we explored the effects of CT-1 on NRBCs *in vitro*. The results ruled out CT-1 directly participating in NRBC infiltration (Figure S3), but suggested that CT-1 induces NRBC transition toward CMs, which is invalid in the blood. In this study, the maximum concentrations of CT-1 in cardiac homogenate and serum of 30 dac were respectively 53 fmol mg^{-1} and 163 fM. It is difficult to measure CT-1 in cardiac interstitial fluid. Our preparatory experiment showed that hCT-1 at 0.2 nM had no influence on NRBCs. One study reports that hCT-1 at 10 ng mL^{-1} (≈0.5 nM) induced human cardiac fibroblast transdifferentiation to myofibroblasts. Accordingly, 0.5 nM hCT-1 was used here. CT-1 induced NRBC transdifferentiation toward CMs, but the transdifferentiation stopped at cell death. The cell death might be caused by one of the following reasons: ① The transition required an increasingly rigorous microenvironment, which was not satisfied by the given conditions; ② the role of CT-1 in the transition is limited.[73]

In summary, this study proposes NRBCs as a cell source for CM renewal/regeneration in adult vertebrates: CM loss triggers NRBC infiltration and transition to CMs; NRBC infiltration pause due to NRBC supply suspension delays myocardial regeneration. This finding implies that a lack of NRBCs might be a reason for the limited human heart regeneration. Utilization of bone marrow NRBCs might enhance human myocardial regeneration.

Limitations and future perspective

The whole process of NRBCs transdifferentiation into CMs was not directly observed in this study. To make the study conclusion solid, the following two experiments should be performed separately or in combination: after cardiac cautery, local implantation of NRBCs to accelerate neomyocardium formation; after cardiac cautery, local implantation or systemic transplantation of gene-labeled NRBCs to observe the NRBC participation in the formation of new myocardium dynamically.

AUTHORS' CONTRIBUTIONS

SQL conceived and designed the study. All authors participated in implementation of the experiments, analysis of the data and review of the manuscript. SQL and XYH wrote the manuscript.

ACKNOWLEDGMENTS

The authors thank Dr. Kai Wang at Department of Pathology, First Affiliated Hospital, Xi'an Jiaotong University, and Mr. Jian-Li He at The Center for Medical Testing, Xi'an Jiaotong University, for technical helps.

DECLARATION OF CONFLICTING INTERESTS

The author(s) declared no potential conflicts of interest with respect to the research, authorship, and/or publication of this article.

FUNDING

The author(s) disclosed receipt of the following financial support for the research, authorship, and/or publication of this article: The work was supported by Xi'an Jiaotong University Free Exploration and Independent Innovation Project [XJJ2012055].

ORCID iD

Shu-Qin Liu https://orcid.org/0000-0001-8760-7304

Supplemental material

Supplemental material for this article is available online.

REFERENCES

1. González-Rosa JM, Burns CE, Burns CG. Zebrafish heart regeneration: 15 years of discoveries. *Regeneration* 2017;**4**:105–23
2. Sakaguchi A, Nishiyama C, Kimura W. Cardiac regeneration as an environmental adaptation. *Biochim Biophys Acta Mol Cell Res* 2020;**1867**:118623
3. Aix E, Gutiérrez-Gutiérrez Ó, Sánchez-Ferrer C, Aguado T, Flores I. Postnatal telomere dysfunction induces cardiomyocyte cell-cycle arrest through p21 activation. *J Cell Biol* 2016;**213**:571–83
4. Zebrowski DC, Jensen CH, Becker R, Ferrazzi F, Baun C, Hvidsten S, Sheikh SP, Polizzotti BD, Andersen DC, Engel FB. Cardiac injury of the newborn mammalian heart accelerates cardiomyocyte terminal differentiation. *Sci Rep* 2017;**7**:8362
5. Bergmann O, Bhardwaj RD, Bernard S, Zdunek S, Barnabé-Heider F, Walsh S, Zupicich J, Alkass K, Buchholz BA, Druid H, Jovinge S, Frisén J. Evidence for cardiomyocyte renewal in humans. *Science* 2009;**324**:98–102
6. Bergmann O, Zdunek S, Felker A, Salehpour M, Alkass K, Bernard S, Sjostrom SL, Szewczykowska M, Jackowska T, Dos Remedios C, Malm T, Andrä M, Jashari R, Nyengaard JR, Possnert G, Jovinge S, Druid H, Frisén J. Dynamics of cell generation and turnover in the human heart. *Cell* 2015;**161**:1566–75
7. Senyo SE, Steinhauser ML, Pizzimenti CL, Yang VK, Cai L, Wang M, Wu TD, Guerquin-Kern JL, Lechene CP, Lee RT. Mammalian heart renewal by pre-existing cardiomyocytes. *Nature* 2013;**493**:433–6
8. Nakada Y, Canseco DC, Thet S, Abdisalaam S, Asaithamby A, Santos CX, Shah AM, Zhang H, Faber JE, Kinter MT, Szweda LI, Xing C, Hu Z, Deberardinis RJ, Schiattarella G, Hill JA, Oz O, Lu Z, Zhang CC, Kimura W, Sadek HA. Hypoxia induces heart regeneration in adult mice. *Nature* 2017;**541**:222–7
9. Wang WE, Li L, Xia X, Fu W, Liao Q, Lan C, Yang D, Chen H, Yue R, Zeng C, Zhou L, Zhou B, Duan DD, Chen X, Houser SR, Zeng C. Dedifferentiation, proliferation, and redifferentiation of adult mammalian cardiomyocytes after ischemic injury. *Circulation* 2017;**136**:834–48
10. Bargehr J, Ong LP, Colzani M, Davaapil H, Hofsteen P, Bhandari S, Gambardella L, Le Novère N, Iyer D, Sampaziotis F, Weinberger F, Bertero A, Leonard A, Bernard WG, Martinson A, Figg N, Regnier M, Bennett MR, Murry CE, Sinha S. Epicardial cells derived from human embryonic stem cells augment cardiomyocyte-driven heart regeneration. *Nat Biotechnol* 2019;**37**:895–906
11. Hu P, Liu J, Zhao J, Wilkins BJ, Lupino K, Wu H, Pei L. Single-nucleus transcriptomic survey of cell diversity and functional maturation in postnatal mammalian hearts. *Genes Dev* 2018;**32**:1344–57
12. Wolfien M, Galow AM, Müller P, Bartsch M, Brunner RM, Goldammer T, Wolkenhauer O, Hoeflich A, David R. Single-nucleus sequencing of an entire mammalian heart: cell type composition and velocity. *Cell* 2020;**9**:318
13. Xinyun C, Zhi Z, Bin Z, Li R, Yucheng C, Yafei Y, Tingjie Z, Shengfu L. Effects of cardiotrophin-1 on differentiation and maturation of rat bone marrow mesenchymal stem cells induced with 5-azacytidine in vitro. *Int J Cardiol* 2010;**143**:171–7
14. Mekala SR, Wörsdörfer P, Bauer J, Stoll O, Wagner N, Reeh L, Loew K, Eckner G, Kwok CK, Wischmeyer E, Dickinson ME, Schulze H, Stegner D, Benndorf RA, Edenhofer F, Pfeiffer V, Kuerten S, Frantz S, Ergün S. Generation of cardiomyocytes from vascular adventitia-resident stem cells. *Circ Res* 2018;**123**:686–99
15. Rajabzadeh N, Fathi E, Farahzadi R. Stem cell-based regenerative medicine. *Stem Cell Investig* 2019;**6**:19
16. Fathi E, Farahzadi R, Vietor I, Javanmardi S. Cardiac differentiation of bone-marrow-resident c-kit^{+} stem cells by L-carnitine increases through secretion of VEGF, IL6, IGF-1, and TGF- β as clinical agents in cardiac regeneration. *J Biosci* 2020;**45**:92
17. Fathi E, Farahzadi R, Javanmardi S, Vietor I. L-carnitine extends the telomere length of the cardiac differentiated CD117^{+}-expressing stem cells. *Tissue Cell* 2020;**67**:101429
18. Zarniko N, Skorska A, Steinhoff G, David R, Gaebel R. Dose-independent therapeutic benefit of bone marrow stem cell transplantation after MI in mice. *Biomedicines* 2020;**8**:157
19. Mathison M, Singh VP, Chiuchiolo MJ, Sanagasetti D, Mao Y, Patel VB, Yang J, Kaminsky SM, Crystal RG, Rosengart TK. In situ reprogramming to transdifferentiate fibroblasts into cardiomyocytes using adenoviral vectors: implications for clinical myocardial regeneration. *J Thorac Cardiovasc Surg* 2017;**153**:329–39
20. Mohamed TM, Stone NR, Berry EC, Radzinsky E, Huang Y, Pratt K, Ang YS, Yu P, Wang H, Tang S, Magnitsky S, Ding S, Ivey KN, Srivastava D. Chemical enhancement of in vitro and in vivo direct cardiac reprogramming. *Circulation* 2017;**135**:978–95
21. Flink IL. Cell cycle reentry of ventricular and atrial cardiomyocytes and cells within the epicardium following amputation of the ventricular apex in the axolotl, amblystoma mexicanum: confocal microscopic immunofluorescent image analysis of bromodeoxyuridine-labeled nuclei. *Anat Embryol* 2002;**205**:235–44
22. Lafontant PJ, Burns AR, Grivas JA, Lesch MA, Lala TD, Reuter SP, Field LJ, Frounfelter TD. The giant danio (D. aequipinnatus) as a model of cardiac remodeling and regeneration. *Anat Rec* 2012;**295**:234–48
23. Grivas J, Haag M, Johnson A, Manalo T, Roell J, Das TL, Brown E, Burns AR, Lafontant PJ. Cardiac repair and regenerative potential in the goldfish (Carassius auratus) heart. *Comp Biochem Physiol C Toxicol Pharmacol* 2014;**163**:14–23
24. Liao S, Dong W, Lv L, Guo H, Yang J, Zhao H, Huang R, Yuan Z, Chen Y, Feng S, Zheng X, Huang J, Huang W, Qi X, Cai D. Heart regeneration in adult xenopus tropicalis after apical resection. *Cell Biosci* 2017;**7**:70
25. Piatkowski T, Muhlfeld C, Borchardt T, Braun T. Reconstitution of the myocardium in regenerating newt hearts is preceded by transient deposition of extracellular matrix components. *Stem Cells Dev* 2013;**22**:1921–31
26. Hermansen MC. Nucleated red blood cells in the fetus and newborn. *Arch Dis Child Fetal Neonatal Ed* 2001;**84**:F211–5
27. Hu G, Guan R, Li L. Nucleated red blood cell count in maternal peripheral blood and hypertensive disorders in pregnant women. *Am J Med Sci* 2016;**351**:140–6
28. Danise P, Maconi M, Barrella F, Di PA, Avino D, Rovetti A, Gioia M, Amendola G. Evaluation of nucleated red blood cells in the peripheral blood of hematological diseases. *Clin Chem Lab Med* 2011;**50**:357–60
29. Desai S, Jones SL, Turner KL, Hall J, Moore LJ. Nucleated red blood cells are associated with a higher mortality rate in patients with surgical sepsis. *Surg Infect* 2012;**13**:360–5
30. Lam NT, Sadek HA. Neonatal heart regeneration: comprehensive literature review. *Circulation* 2018;**138**:412–23
31. Mahmoud AI, Porrello ER. Upsizing neonatal heart regeneration. *Circulation* 2018;**138**:2817–9
32. Velayutham N, Agnew EJ, Yutzey KE. Postnatal cardiac development and regenerative potential in large mammals. *Pediatr Cardiol* 2019;**40**:1345–58
33. Eghbali M, Deva R, Alioua A, Minosyan TY, Ruan H, Wang Y, Toro L, Stefani E. Molecular and functional signature of heart hypertrophy during pregnancy. *Circ Res* 2005;**96**:1208–16
34. Minior VK, Levine B, Ferber A, Guller S, Divon MY. Nucleated red blood cells as a marker of acute and chronic fetal hypoxia in a rat model. *Rambam Maimonides Med J* 2017;**8**:e0025
35. Luban NL, Kapur S, DePalma L. Pericardial extramedullary hematopoiesis in a neonate with congenital heart disease: a case report. *Acta Cytol* 1993;**37**:729–31
36. Goldman BI, Wurzel J. Hematopoiesis/erythropoiesis in myocardial infarcts. *Mod Pathol* 2001;**14**:589–94
37. Farhi DC. *Bone marrow structure, morphology, and hematopoiesis, erythroid cells. Pathology of bone marrow and blood cells*. 2nd ed. Philadephia: Wolters Kluwer/Lippincott Williams & Wilkins, 2008, p. 11
38. Hadji-Azimi I, Coosemans V, Canicatti C. Atlas of adult *Xenopus laevis laevis* hematology. *Dev Comp Immunol* 1987;**11**:807–74
39. Liu SQ, Li ZL, Cao YX, Li L, Ma X, Zhao XG, Kang AQ, Liu CH, Yuan BX. Transfusion of autologous late-outgrowth endothelial cells reduces arterial neointima formation after injury. *Cardiovasc Res* 2011;**90**:171–81
40. Liu CB, Li RD. Electrocardiogram and heart rate in response to temperature acclimation in three representative vertebrates. *Comp Biochem Physiol A Mol Integr Physiol* 2005;**142**:416–21

41. Mačianskienė R, Martišienė I, Navalinskas A, Vosyliūtė R, Treinys R, Vaidelytė B, Benetis R, Jurevičius J. Evaluation of excitation propagation in the rabbit heart: optical mapping and transmural microelectrode recordings. *PLoS One* 2015;**10**:e0123050
42. Xie J, Zhang Y, Wang L, Qi W, Zhang M. Composition of fatty oils from semen ziziphi spinosae and its cardiotonic effect on isolated toad hearts. *Nat Prod Res* 2012;**26**:479–83
43. Fathi E, Valipour B, Sanaat Z, Nozad Charoudeh H, Farahzadi R. Interleukin-6, -8, and TGF-β secreted from mesenchymal stem cells show functional role in reduction of telomerase activity of leukemia cell via Wnt5a/β-catenin and P53 pathways. *Adv Pharm Bull* 2020;**10**:307–14
44. Müller P, Lemcke H, David R. Stem cell therapy in heart diseases - cell types, mechanisms and improvement strategies. *Cell Physiol Biochem* 2018;**48**:2607–55
45. Mohsin S, Siddiqi S, Collins B, Sussman MA. Empowering adult stem cells for myocardial regeneration. *Circ Res* 2011;**109**:1415–28
46. Dimmeler S, Zeiher AM. Cell therapy of acute myocardial infarction: open questions. *Cardiology* 2009;**113**:155–60
47. Matar AA, Chong JJ. Stem cell therapy for cardiac dysfunction. *SpringerPlus* 2014;**3**:440
48. Honold J, Fischer-Rasokat F, Seeger FH, Leistner D, Lotz S, Dimmeler S, Zeiher AM, Assmus B. Impact of intracoronary reinfusion of bone marrow-derived mononuclear progenitor cells on cardiopulmonary exercise capacity in patients with chronic postinfarction heart failure. *Clin Res Cardiol* 2013;**102**:619–25
49. Sasse S, Skorska A, Lux CA, Steinhoff G, David R, Gaebel R. Angiogenic potential of bone marrow derived $CD133^+$ and $CD271^+$ intramyocardial stem cell transplantation post MI. *Cells* 2019;**9**:78
50. Kim H, Kim S, Baek SH, Kwon SM. Pivotal cytoprotective mediators and promising therapeutic strategies for endothelial progenitor cell-based cardiovascular regeneration. *Stem Cells Int* 2016;**2016**:8340257
51. Van Berlo JH, Kanisicak O, Maillet M, Vagnozzi RJ, Karch J, Lin S-CJ, Middleton RC, Marbán E, Molkentin JC. Kit+ cells minimally contribute cardiomyocytes to the heart. *Nature* 2014;**509**:337–41
52. Afzal MR, Samanta A, Shah ZI, Jeevanantham V, Abdel-Latif A, Zuba-Surma EK, Dawn B. Adult bone marrow cell therapy for ischemic heart disease: evidence and insights from randomized controlled trials. *Circ Res* 2015;**117**:558–75
53. Boutilier RG, Toews DP. Respiratory, circulatory and acid-base adjustments to hypercapnia in a strictly aquatic and predominantly skin-breathing urodele, cryptobranchus alleganiensis. *Respir Physiol* 1981;**46**:177–92
54. de Abreu Manso PP, de Brito-Gitirana L, Pelajo-Machado M. Localization of hematopoietic cells in the bullfrog (lithobates catesbeianus). *Cell Tissue Res* 2009;**337**:301–12
55. Cano-Martínez A, Vargas-González A, Guarner-Lans V, Prado-Zayago E, León-Oleda M, Nieto-Lima B. Functional and structural regeneration in the axolotl heart (ambystoma mexicanum) after partial ventricular amputation. *Arch Cardiol Mex* 2010;**80**:79–86
56. Witman N, Murtuza B, Davis B, Arner A, Morrison JI. Recapitulation of developmental cardiogenesis governs the morphological and functional regeneration of adult newt hearts following injury. *Dev Biol* 2011;**354**:67–76
57. Ito K, Morioka M, Kimura S, Tasaki M, Inohaya K, Kudo A. Differential reparative phenotypes between zebrafish and medaka after cardiac injury. *Dev Dyn* 2014;**243**:1106–15
58. Marshall L, Vivien C, Girardot F, Péricard L, Demeneix BA, Coen L, Chai N. Persistent fibrosis, hypertrophy and sarcomere disorganisation after endoscopy-guided heart resection in adult xenopus. *PLoS One* 2017;**12**:e0173418
59. Stockdale WT, Lemieux ME, Killen AC, Zhao J, Hu Z, Riepsaame J, Hamilton N, Kudoh T, Riley PR, van Aerle R, Yamamoto Y, Mommersteeg MTM. Heart regeneration in the Mexican cavefish. *Cell Rep* 2018;**25**:1997–2007
60. Kikuchi K, Holdway JE, Major RJ, Blum N, Dahn RD, Begemann G, Poss KD. Retinoic acid production by endocardium and epicardium is an injury response essential for zebrafish heart regeneration. *Dev Cell* 2011;**20**:397–404
61. Fujio Y, Maeda M, Mohri T, Obana M, Iwakura T, Hayama A, Yamashita T, Nakayama H. Glycoprotein 130 cytokine signal as a therapeutic target against cardiovascular diseases. *J Pharmacol Sci* 2011;**117**:213–22
62. Yoshida K, Taga T, Saito M, Suematsu S, Kumanogoh A, Tanaka T, Fujiwara H, Hirata M, Yamagami T, Nakahata T, Hirabayashi T, Yoneda Y, Tanaka K, Wang WZ, Mori C, Shiota K, Yoshida N, Kishimoto T. Targeted disruption of gp130, a common signal transducer for the interleukin 6 family of cytokines, leads to myocardial and hematological disorders. *Proc Natl Acad Sci U S A* 1996;**93**:407–11
63. Brandt C, Pedersen BK. The role of exercise-induced myokines in muscle homeostasis and the defense against chronic diseases. *J Biomed Biotechnol* 2010;**2010**:520258
64. Kong P, Christia P, Frangogiannis NG. The pathogenesis of cardiac fibrosis. *Cell Mol Life Sci* 2014;**71**:549–74
65. Schafer S, Viswanathan S, Widjaja AA, Lim WW, Moreno-Moral A, DeLaughter DM, Ng B, Patone G, Chow K, Khin E, Tan J, Chothani SP, Ye L, Rackham OJL, Ko NSJ, Sahib NE, Pua CJ, Zhen NTG, Xie C, Wang M, Maatz H, Lim S, Saar K, Blachut S, Petretto E, Schmidt S, Putoczki T, Guimarães-Camboa N, Wakimoto H, van Heesch S, Sigmundsson K, Lim SL, Soon JL, Chao VTT, Chua YL, Tan TE, Evans SM, Loh YJ, Jamal MH, Ong KK, Chua KC, Ong BH, Chakaramakkil MJ, Seidman JG, Seidman CE, Hubner N, Sin KYK, Cook SA. IL-11 is a crucial determinant of cardiovascular fibrosis. *Nature* 2017;**552**:110–5
66. Aitsebaomo J, Srivastava S, Zhang H, Jha S, Wang Z, Winnik S, Veleva AN, Pi X, Lockyer P, Faber JE, Patterson C, Patterson C. Recombinant human interleukin-11 treatment enhances collateral vessel growth after femoral artery ligation. *Arterioscler Thromb Vasc Biol* 2011;**31**:306–12
67. Jougasaki M. Cardiotrophin-1 in cardiovascular regulation. *Adv Clin Chem* 2010;**52**:41–76
68. Mascheck L, Sharifpanah F, Tsang SY, Wartenberg M, Sauer H. Stimulation of cardiomyogenesis from mouse embryonic stem cells by nuclear translocation of cardiotrophin-1. *Int J Cardiol* 2015;**193**:23–33
69. Liu G, Li L, Huo D, Li Y, Wu Y, Zeng L, Cheng P, Xing M, Zeng W, Zhu C. A VEGF delivery system targeting MI improves angiogenesis and cardiac function based on the tropism of MSCs and layer-by-layer self-assembly. *Biomaterials* 2017;**127**:117–31
70. Giannelli G, Falk-Marzillier J, Schiraldi O, Stetler-Stevenson WG, Quaranta V. Induction of cell migration by matrix metalloprotease-2 cleavage of laminin-5. *Science* 1997;**277**:225–8
71. Mook OR, Frederiks WM, Van Noorden CJ. The role of gelatinases in colorectal cancer progression and metastasis. *Biochim Biophys Acta* 2004;**1705**:69–89
72. McQuibban GA, Gong JH, Tam EM, McCulloch CA, Clark-Lewis I, Overall CM. Inflammation dampened by gelatinase a cleavage of monocyte chemoattractant protein-3. *Science* 2000;**289**:1202–6
73. López B, González A, Querejeta R, Larman M, Rábago G, Díez J. Association of cardiotrophin-1 with myocardial fibrosis in hypertensive patients with heart failure. *Hypertension* 2014;**63**:483–9

(Received December 4, 2020, Accepted April 8, 2021)